Scanning near-field optical microscopy based on the heterodyne phase-controlled oscillator method

G. T. Shubeita, S. K. Sekatskii,[a] B. Riedo, and G. Dietler
Institut de Physique de la Matière Condensée, Université de Lausanne, BSP, CH1015 Lausanne-Dorigny, Switzerland

U. Dürig
Zurich Research Laboratory, IBM Research Division, CH8803 Rüschlikon, Switzerland

(Received 13 March 2000; accepted for publication 23 May 2000)

The heterodyne phase-controlled oscillator method to monitor the resonance frequency and quality factor of the tip oscillations was used to control the scanning near-field optical microscope (SNOM) and to study the nature of the shear-force interaction routinely used in SNOM. Both optical and nonoptical (tuning fork-based) detection schemes of the shear force have been investigated using the same electronic unit, which enables a direct comparison of the results. It is shown that the possibility to record simultaneously the topography and dissipative interaction (Q-factor) channels gives additional information about the sample and helps to interpret the data in a manner analogous to that of a usual dynamic force microscope. The peculiarities of the recorded approach curves (increase of the resonance frequency and Q factor when the tip approaches the sample) are consistent with the ''repetitive bumping'' mechanism of tip–sample interaction for the shear force. Evidence for the transition from the bumping to the permanent sliding mechanism has been obtained for the case of larger vibration amplitudes of the tip. © *2000 American Institute of Physics.* [S0021-8979(00)04017-2]

I. INTRODUCTION

Scanning near-field optical microscopy (SNOM) is increasingly becoming a routinely used method in nanotechnology and biology. Soon after the first experiments, sharpened optical fibers appeared as the most commonly used sensor in the field of near-field optics because of their broad availability, low cost, excellent optical properties and easiness to handle. At the same time, the particular mechanical properties of such a ''lever'' prevented the broad use of the force-measurement and feedback schemes usually employed in atomic force microscopy (AFM),[1] and novel feedback schemes to operate with fiber-equipped SNOM had to be elaborated.

The shear-force method to regulate the tip–sample distance in the SNOM was first proposed in 1992,[2] and is at present the most commonly used technique in the field. The idea behind the method is based on the measurement of the damping of the oscillation of the tip subject to nanometer lateral dithering when approaching the sample surface. First, optical detection schemes to control the amplitude and/or phase of the lateral oscillations of the tip were utilized, but nonoptical detection schemes were soon introduced,[3,4] and among them the scheme employing the attachment of the sharpened fiber to a high Q piezoelectric tuning fork[3] became very popular in the recent years.

However, although most of the SNOM experiments are performed exploiting the shear force, the exact nature of the force is still unclear. Initially, pure dissipative viscous forces and other unknown forces between the tip and the contaminated sample surface (covered with a water layer) have been invoked as an explanation for the nature of the shear force[2,3] in close analogy with atomic force microscopy.[5] Recent work aimed at investigating the shear force as a function of humidity and sample and surface hydrophobicity[6] confirms this picture under certain conditions. Recently, it has been shown that shear forces exist also in ultrahigh vacuum (UHV) at liquid helium temperature conditions,[7] and the mechanism of normal collisions between the tip and the sample, somewhat analogous to the tapping mode in AFM,[5] has been introduced to explain the nature of the shear force[7] (some inclination of the tip with respect to the surface normal always exists in a real experiment). This model has been confirmed also by experiments using combined shear-force and scanning tunneling microscope (STM) signal measurements:[8,9] shear-force damping exists only simultaneously with the electrical current between the tip and the sample, and thus its existence is a result of ''real'' tip–sample contact (bumping).

Obviously these uncertainties make the interpretation of SNOM results difficult and sometimes rather unclear. Further investigations on the nature of the shear force are necessary. Generally speaking, measuring only the amplitude and/or phase of the lateral tip vibrations is not sufficient and additional information about the interaction is required. The situation is even more complicated because of the aforementioned coexistence of optical and nonoptical shear-force detection schemes. The main parameters of tip–sample interactions (oscillation amplitude, Q factor, etc.) are rather different for both schemes, thus different electronic units are

[a]Electronic mail: sergey.sekatskii@impc.unil.ch

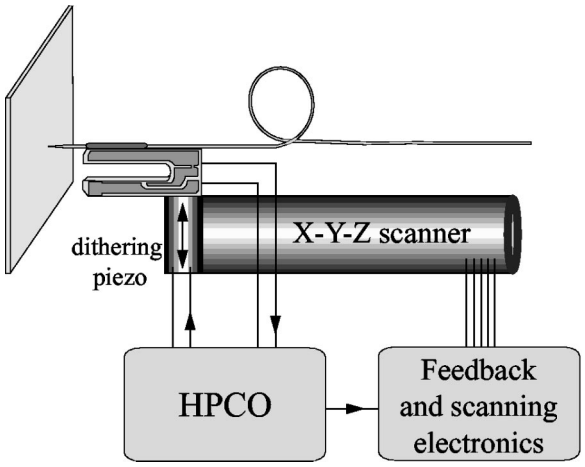

FIG. 1. Schematic diagram of the shear-force distance regulation scheme based on a tuning fork (nonoptical detection). The HPCO maintains driving the fiber glued to the tuning fork at its resonance frequency as it interacts with the sample. The signal generated on the piezoelectrical tuning fork serves as input to the HPCO.

usually used which makes the comparison of the results especially difficult.

We proposed that the necessary additional information can be gained using dynamical force microscopy with the simultaneous measurement of the two main parameters of the tip oscillations, namely, the resonance frequency ω and the quality factor Q, as has been already described and realized for the AFM.[10–12]

Results of such an approach are discussed in the present work. The resonance frequency ω and the quality factor Q were obtained using a heterodyne phase-controlled oscillator (HPCO). It has been shown that such a dynamic force monitoring method can be successfully used to regulate the tip–sample distance and obtain additional information about the sample surface. The same electronic unit was used to monitor the tip–sample interaction parameters for both optical and nonoptical schemes of the shear-force measurement, which enables the study of the force in a broad range of experimental parameters and gives the possibility of a direct comparison of the results.

II. EXPERIMENTS

A. Scanning near-field optical microscope equipped with the heterodyne phase-controlled oscillator electronic unit

The experiments were performed using a homemade SNOM exploited earlier for the investigation of SNOM-related fluorescence resonance energy transfer.[13] First we discuss the experimental results obtained using the nonoptical detection scheme.

The experimental setup is presented in Fig. 1. The sharpened tip with a radius of curvature of 100–200 nm (homemade tips as well as the tips supplied by Nanonics Supertips, Israel, were used; no material difference between different types of fibers was revealed) was glued by a drop of rosin along the side of one of the prongs of a quartz crystal tuning fork (Farnell Components; resonance frequency 32 768 Hz)

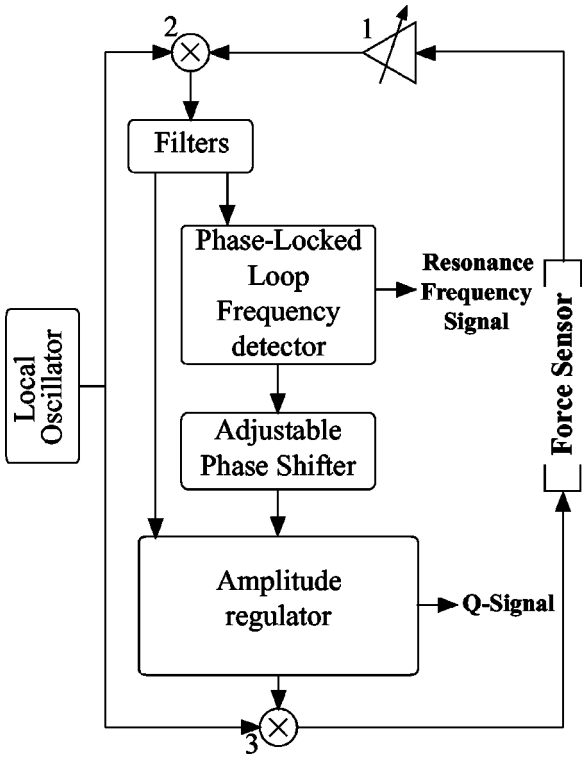

FIG. 2. Schematic diagram of the heterodyne phase-controlled oscillator. 1—Input amplifier, 2—input mixer, 3—single sideband output mixer.

in such a manner that a 1–2 mm long piece of the fiber remained free. The fork was then glued on the top of a piezocylinder, which was used to excite the resonant vibrations of the fork. The quality factor, which is equal to 7500 for the free tuning fork operating in air, decreased to a typical value of ~ 150 after gluing the fiber while the resonance frequency decreased by a value of ~ 400 Hz. The piezoelectric signal from the tuning fork was preamplified and then used as input for the heterodyne phase-controlled oscillator electronic unit.[14]

A block diagram of the HCPO electronic unit is shown in Fig. 2. Its detailed description can be found in Ref. 12 and will not be repeated here. Briefly, this scheme is a practical realization of the oscillator method of dynamic force microscopy, where the force sensor acts as a resonator in an active feedback circuit. The input signal is converted to a signal with the intermediate frequency of 35 kHz. The interaction-related change of the resonance frequency is measured by a phase locked loop (PLL) frequency detector with a sensitivity of 0.2 Hz_{rms} at a bandwidth of 1 kHz, and with a linearity error of less than 0.05%.

The amplitude regulator, by processing the intermediate frequency signal and the PLL phase detector signal, forms the signal to excite the force sensor. The output signal of the amplitude regulator is then converted to the resonance frequency by means of a single sideband mixer employing the phase method. The amplitude of the excitation signal is electronically adjusted in such a manner that at resonance the fiber oscillation amplitude is kept constant. The mean amplitude of the driving voltage is inversely proportional to the Q

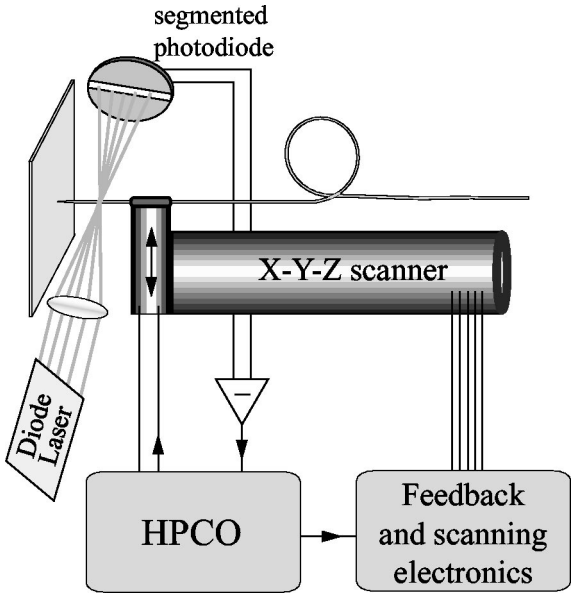

FIG. 3. Schematic diagram of the optical scheme for shear-force distance regulation. The signal from the segmented photodiode, due to the laser light scattered by the dithering fiber, is used as input to the HPCO, which in turn drives the piezotube to maintain oscillating the fiber at its resonance frequency.

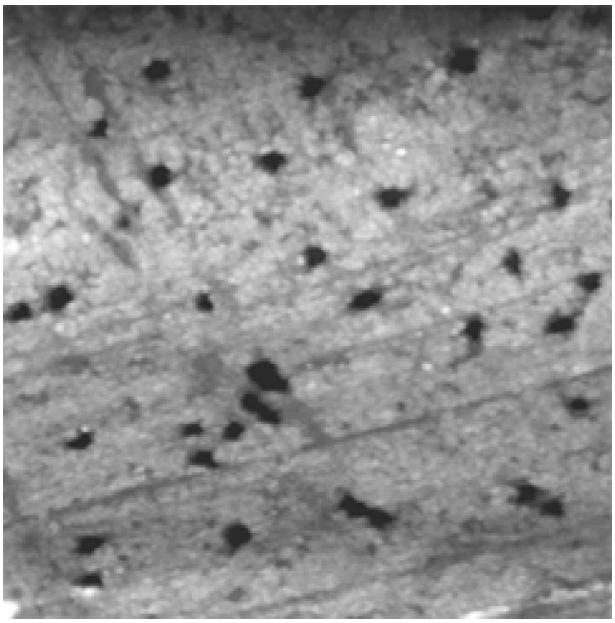

FIG. 4. Tapping-mode AFM image of a nuclear filter having holes with mean size of 25 nm (scan size: 1×1 μm^2).

factor, and a corresponding signal is available as an independent output of the amplitude regulator.

The dynamic range of the HPCO is 10 kHz, with a maximum phase error of less than 2% over the entire range, and a response time around 0.1 ms can be achieved. In brief, this HPCO scheme enables a fast, precise, and *Q*-independent measurement of the oscillator resonance frequency as well as a fast and precise relative measurement of the *Q* factor. Both ω and *Q* signals are available at the output of the scheme in the form of dc voltage, and both of them can be simultaneously recorded and/or used as a control parameter to regulate the tip–sample distance.

Thus, two operation modes are possible: (i) one can use the frequency signal as a feedback setpoint (constant frequency mode) while recording the *Q* factor and topography (*z*-coordinate driving voltage) signals; and (ii) one can use the quality factor-related signal as a feedback setpoint (constant *Q* mode) while recording the frequency and topography signals. Of course, the near-field optical signal for any of the known SNOM operation modes (collection, transmission or reflection) can be additionally recorded. Obviously these images contain complementary information, although their full interpretation, as in the case of dynamic force AFM, is not easily obtained. Nevertheless, the main peculiarities are known: the resonance frequency is mainly related to the mean force gradient while the *Q* factor is mainly related to the mean dissipation force,[10–12,15] and thus we call the operation modes mentioned earlier constant force gradient mode and constant mean dissipation force mode, respectively.

The same HPCO electronic unit was used to monitor the resonance frequency and *Q* factor for the lateral tip oscillations recorded with an optical detection scheme (Fig. 3). For such an approach, a sharpened tip was glued by a drop of rosin directly to the top of the dithering piezocylinder in such a manner that a 3–4 mm long piece of the fiber remained free. The amplitude of the lateral dithering of the tip was controlled by monitoring the scattering of the focused laser light with a two-sector photodiode.[2] The first resonance frequency of the lateral dithering (ranging from 12 to 30 kHz) has been used. The measured *Q* factor ranged from 40 to 100. The signal from the photodiode was preamplified and then used as the input for the HPCO electronic unit.

B. Topographical, constant dissipation and near-field optical images

Both the aforementioned possible operation modes of the HCPO-based SNOM were implemented practically for optical and nonoptical detection schemes. In all cases stable performance of the SNOM has been attained, and high quality and highly contrasted optical images of different samples (fragments of nuclear filters and a CD-ROM) were obtained.

Nuclear filters are thin (5–20 μm thick) lavsan (polyethylene terephtalate) films containing holes with sizes ranging from ten nanometers to tens of microns produced by high energy ion irradiation and subsequent chemical treatment.[16] Different nuclear filter samples with mean hole sizes of 500, 200 and 25 nm were obtained from the Joint Institute of Nuclear Studies (Dubna, Russia) and were tested as prospective test objects for the SNOM and AFM.[17] A ''tapping-mode''[5] AFM image of a nuclear filter sample with the mean hole size of 25 nm is presented in Fig. 4.

To illustrate the performance of our SNOM, in Fig. 5 we present a near-field optical image (light collection mode) of a nuclear filter coated with a 30 nm thick gold layer. Single holes are well seen in this image as bright spots.[18] Analysis of similar images enables us to estimate the spatial resolution of the microscope as somewhat better than 100 nm, which is consistent with the size of the tip aperture (100–200 nm).

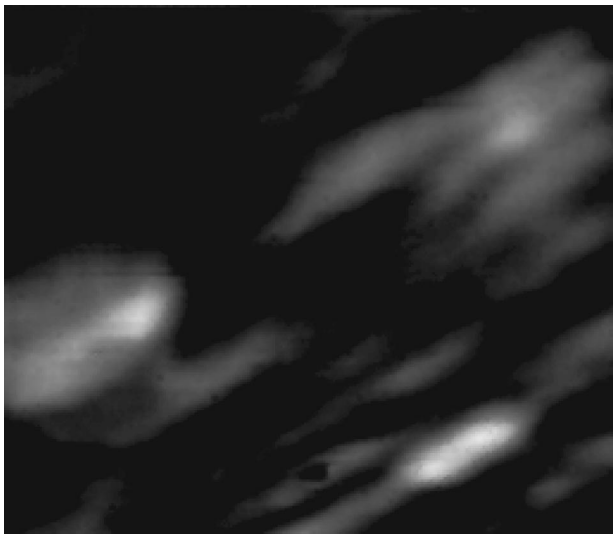

FIG. 5. Near-field optical image of a gold-coated nuclear filter having the mean pore size of 500 nm. A HeNe laser was used to image (the gold layer thickness was 30 nm, and the scan size was $7\times6\ \mu m^2$).

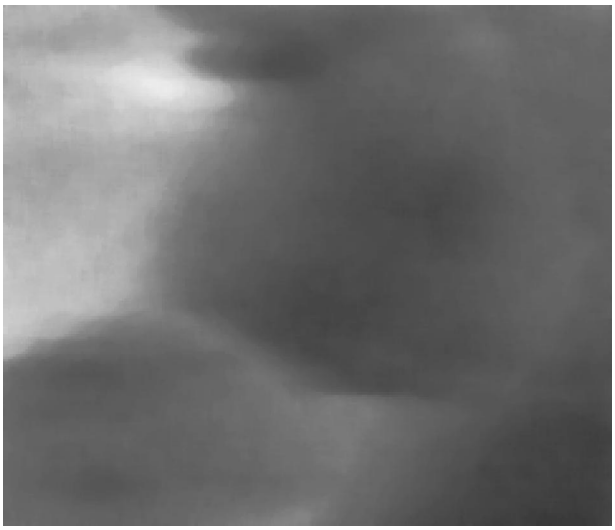

FIG. 7. Quality factor image of a gold-coated polymer film recorded with the optical scheme-based HPCO. ''Grains'' of different elastic properties are probably imperfections in the metal coating (scan size: $6.7\times5.7\ \mu m^2$).

Stable operation of the SNOM was routine in the tuning fork-based shear-force distance regulation scheme using the HPCO. Figure 6 shows an image of a portion of a CD-ROM surface acquired with the resonance frequency shift used for feedback regulation [thus Fig. 6(c) represents the image obtained with the feedback error signal[5]]. The topography image [Fig. 6(a)] reveals a depression in the surface which proved to be a hole as seen by the increased light intensity in that region in the near-field optical image acquired in collection mode [Fig. 6(d)]. (For this particular image CD stripes are practically unseen in the optical image due to the very bright light passing through the depression, but it should be noted that such stripes were contrasted, although faintly, even when imaged with uncoated fiber tips.) The quality factor images were the most contrasted and the most informative ones in comparison with the other types of recorded images. For example, the *Q*-factor image of Fig. 6(b) reveals highly contrasted fine structures which carry complementary information: one of the CD stripes (shown by the arrow in Fig. 6(b)] is seen as partly torn and ''dangling'' over the hole much more convincingly in this image than in the other three. This is consistent with the observations made in the dynamic force AFM practice: such dissipation images contain additional information about the distribution of plasto-mechanical properties of the sample.[12]

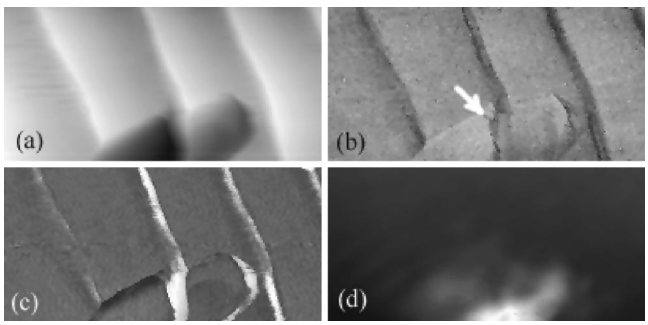

FIG. 6. A $2.6\times5.5\ \mu m^2$ scan of a CD-ROM surface using the nonoptical HPCO-controlled shear-force scheme for distance regulation. (a) Topography; (b) quality factor; (c) resonance frequency; (d) near-field optical image.

We did not record any images with the same high resolution when working in constant-*Q* mode and recording the resonance frequency shift. A simple analysis of a damped oscillator indicates that the *Q* factor is much more sensitive to the interaction details than the resonance frequency.[5] From a practical point of view, it should be noted that the SNOM performance in constant-*Q* operation mode was very stable while the measured $\Delta\omega$ values were very small (<50 Hz). Thus, such an operation mode seems preferable when an extremely small force gradient is acting.

Both constant frequency and constant *Q*-factor modes of operation were also investigated with the optical shear-force distance regulation scheme. General conclusions about this scheme are similar to those mentioned above in connection with the nonoptical detection scheme. However, stable operation of the microscope in constant frequency mode was more difficult to achieve, and stable operation was only possible in a rather narrow range of resonance frequency shifts. The topographical feedback signal recorded for constant frequency SNOM operation mode was usually almost structureless, while the *Q* signal indeed often revealed additional structure. For example, the ''grain'' structure, which is absent in the topography image and we believe is an imperfection of the metal coating of the nuclear filter polymer film (the scanned area does not contain holes), is seen in Fig. 7.

The positive frequency shift corresponding to the repulsive tip–sample interactions[5] has been recorded for both optical and nonoptical detection schemes. The worse performance of the optical detection scheme in comparison with the non-optical one is due to the essentially larger amplitude of oscillations *A* in the former case (100–200 nm and a few nanometers, respectively). It follows from a theoretical analysis[15] that the frequency shift in dynamic-force microscopy at constant mean tip–sample distance *d* is proportional to $A^{-3/2}$.

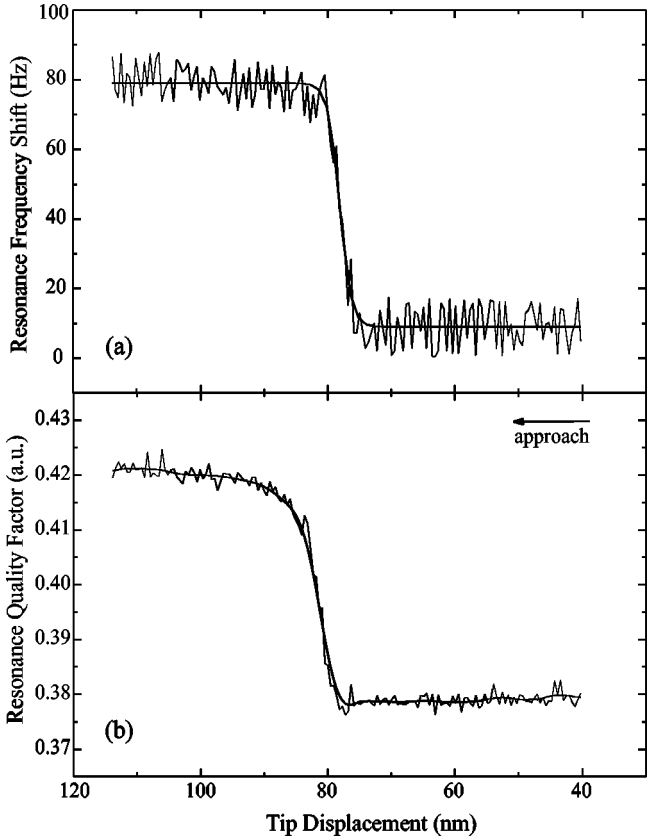

FIG. 8. Approach curves of the fiber tip to a glass slide surface recorded in the nonoptical shear-force detection scheme. (a) The resonance frequency and (b) quality factor were recorded simultaneously, and both increase upon contact.

C. Approach curves: Analysis of the shear force

The typical dependence of the resonance frequency and Q factor of the lateral tip dithering on the mean tip–sample distance during approach to a glass slide surface is shown in Fig. 8 for the tuning fork-based detection scheme. The tip displacement was calculated from the potential difference applied on the piezotube scanner using the coefficient given by the manufacturer: $\zeta = 9.5$ nm/V. From these graphs it is clear that the shear force acts in a very narrow (~ 10 nm) tip–sample distance range, which is consistent with the small tip oscillation amplitude for such a scheme. The positive changes of ω are consistent with the observations of Gregor *et al.*,[7] Atia and Davis,[19] Ruiter *et al.*[20] and some others, and, in our opinion, can be taken as an indication of a ''repetitive bumping'' mechanism of the shear force. An additional fact sustaining the repetitive bumping mechanism is that the measured Q factor increases during approach [Fig. 8(b)]. (Thus, our frequency independent Q-factor measurements contradict observations made in Ref. 20, where only a rather small *decrease* of the Q factor upon approach was reported.)

In a linear approximation (which is justified because the dithering amplitude is always much smaller than the vibrating tip length) the oscillations of the tip or the system tip +fork under the action of an external driving force $F\cos\Omega t$ can be described by the well known equation describing a second-order mechanical system:[21,22]

$$m_{\text{eff}}\ddot{x} + \gamma\dot{x} + kx = F\cos(\Omega t). \tag{1}$$

Here, m_{eff} is an effective oscillator mass, k is the spring constant and γ is the damping constant. For the HCPO approach discussed in the article, the parameters of the excitation are automatically adjusted in such a manner that Ω is equal to the resonance frequency of the system ω, and consequently the values of ω and the quality factor Q at resonance are measured. The quality factor Q for the oscillatory system is[23]

$$Q = \frac{1}{\gamma}\sqrt{km_{\text{eff}}}, \tag{2}$$

and the resonance frequency is

$$\omega = \omega_0\sqrt{1-(1/4Q^2)}, \tag{3}$$

where $\omega_0 = \sqrt{k/m_{\text{eff}}}$ is the resonance frequency for the undamped oscillator; obviously for the case $Q \gg 1$, $\omega \cong \omega_0$.

Both the values of k and γ depend on the mean tip–sample distance and these dependencies define the approach curves for ω and Q. A simple general model for tip–sample interaction consists of using an extra spring constant $\Delta k(z)$ and an extra damping $\Delta\gamma(z)$ appearing as a result of the approach of the tip to the sample surface. Both values of Δk and $\Delta\gamma$ are supposed to be much smaller than k and γ, respectively. If one assumes a purely dissipative interaction force,[2,3] k will be independent of distance while the increase of γ during approach leads, in accordance with Eqs. (2) and (3), to a (rather small and probably unnoticable) decrease of the resonance frequency and a (noticable) decrease of Q. If, however, the damping constant does not change essentially during approach, but the effective spring constant increases due to bumping (because part of the energy is now imparted into mechanical deformation of the tip), then both ω and Q should increase. Figure 8 demonstrates exactly the latter behavior, and thus our experimental results can be considered as confirmation of the repetitive bumping interaction mechanism playing its role in the shear force.

Approach curves recorded using the same fiber tip, but approaching a polymer film rather than a glass slide, showed smaller frequency shifts and quality-factor changes. This is another indication of the sensitivity of the HCPO approach to the local plastomechanical properties of the sample studied, as well as an indication of the importance of the effects of elastic deformations of the sample as a result of the interactions with the tip. Evidently, the elastic deformation of the soft polymer samples is essentially larger than that of glass. Thus, this effect is important for the SNOM as well as for the usual AFM technique where the problem was specially investigated earlier.[24,25]

For similar tip-glass slide surface approach curves recorded using an optical detection scheme (Fig. 9), a more complicated behavior was found. In this case the amplitude of the lateral oscillation was much larger, namely, of the order of $\sim 100-200$ nm. It also should be noted that the optical scattering signal was not of a pure sine wave character (a noticable deviation has been recorded), which made HPCO adjustment and data interpretation more difficult. The resonance frequency of vibrations increased during the ap-

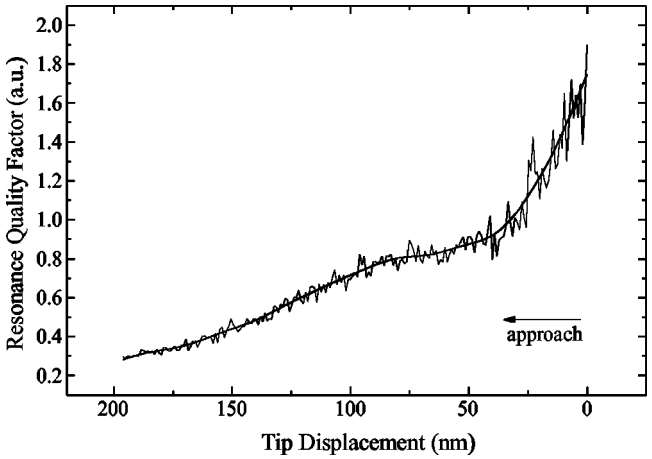

FIG. 9. Quality factor Q during the approach of the fiber tip to a glass slide recorded using the optical shear-force detection scheme. It shows the effect of the large oscillation amplitude.

proach simultaneously with the *decrease* of the Q factor. Thus, both the changes of the spring constant and the damping seem to be important to describe the interaction in this case. Moreover, the approach curves recorded using the optical shear-force detection scheme show different regimes during approach. For example, in Fig. 9, Q decreases more rapidly starting from some point of the approach curve. Sometimes even abrupt (but reproducible) jumps, analogous to that presented in Fig. 10, could be observed.

In our opinion, they can be considered as an indication of the existence of two different regimes of tip–sample interaction for the case where lateral tip oscillations have a large amplitude. Earlier, it has been proposed that the collisions between the tip and sample change to the regime of permanent sliding of the tip along the sample surface when the mean value of the acting force exceeds some critical value[9] (see also Ref. 3).

III. CONCLUSIONS

It has been demonstrated that heterodyne phase-controlled oscillator-based detection of the resonance frequency and Q factor of the lateral tip oscillations can be successfully used for shear-force-based scanning near-field optical microscopy. As in the case of dynamic force AFM, the dissipative channel is closely related to the local tribological properties of the sample surface, and recording of the corresponding images provides additional information which is often necessary for the interpretation of SNOM images.

Simultaneous recording of both ω and Q channels also gives a better understanding of the nature of the shear force routinely used in SNOM, and we believe that the results obtained should be treated as an indication of the repetitive bumping shear-force mechanism. Such information is very important for a number of SNOM applications including, for example, the recently proposed FRET SNOM based on fluorescence resonance energy transfer (FRET) from the tip to the sample which results in improvement of the spatial resolution and sensitivity of SNOM (see Ref. 13, and references therein). The bumping mechanism implies that during the

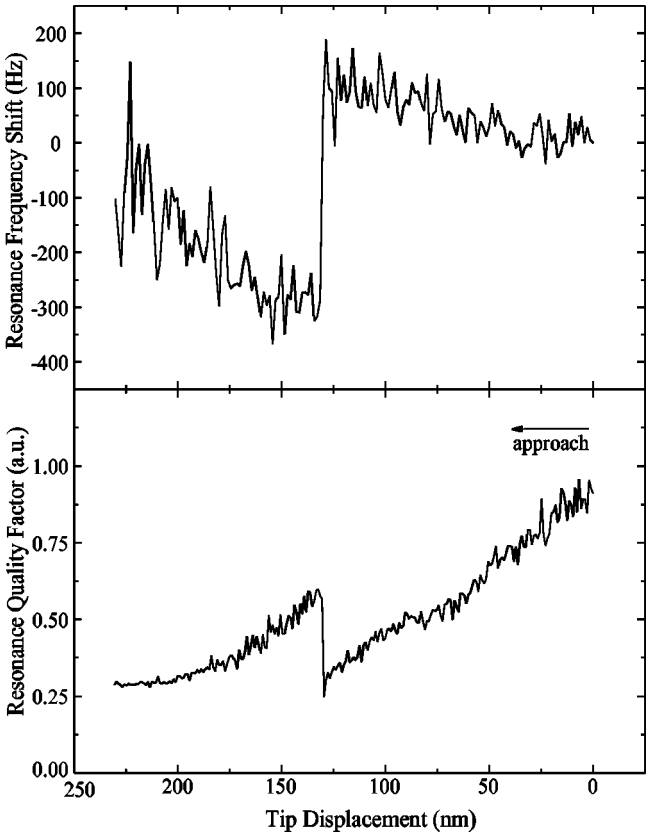

FIG. 10. Resonance frequency and quality factor during the approach of the fiber tip to a glass slide surface, recorded simultaneously with the optical shear-force detection scheme. It shows a probable transition between two regimes of tip–sample interaction.

oscillation direct contact between the tip and the sample takes place, thus enabling a contact phenomenon like FRET to occur. Some kind of a lockin of the optical signal on the frequency of the resonant tip vibrations proves to be very useful to improve the signal to noise ratio when recording such contact interactions.[26]

To conclude, we note that an analogous HPCO approach can be used not only for the shear-force-based SNOM, but also for the normal tip vibration-based SNOM which was demonstrated recently.[27,28]

ACKNOWLEDGMENTS

The authors thank S. G. Zemlyanoi of the Joint Institute of Nuclear Research, Dubna, Russia, for supplying the nuclear filter samples and C. Ramshaw of Cambridge University, UK, for help with the AFM study of these filters. The research was carried out with a partial financial support from the Swiss National Science Foundation, Grant Nos. 2150805.97 and 20-57133.99.

[1] It should be noted that the method to monitor the fiber–tip interaction with the sample using an optical lever with external laser light reflected from a micromirror glued to the bent tip (in a manner similar to usual AFM with soft levers) has been realized but is not broadly accepted; see, for example, C. E. Talley, G. A. Cooksey, and R. Dunn, Appl. Phys. Lett. **69**, 3809 (1996).

[2] R. Toledo-Crow, P. C. Yang, Y. Chen, and M. Vaez-Iravani, Appl. Phys.

Lett. **60**, 2957 (1992); E. Betzig, P. L. Finn, and S. J. Weiner, *ibid.* **60**, 2484 (1992).
[3] K. Karrai and R. D. Grober, Appl. Phys. Lett. **66**, 1842 (1995).
[4] A. Dräbenstedt, J. Wrachtrup, and C. von Borczyskowski, Appl. Phys. Lett. **68**, 3497 (1996); R. Brunner, A. Bietsch, O. Hollricher, and O. Marti, Rev. Sci. Instrum. **68**, 1769 (1997).
[5] D. Sarid, *Scanning Force Microscopy with Applications to Electric, Magnetic, and Atomic Forces*, Oxford Series on Optical Sciences (Oxford University Press, Oxford, 1991).
[6] S. Davy, M. Spajer, and D. Courjon, Appl. Phys. Lett. **73**, 2594 (1998); P. K. Wei and W. S. Fann, J. Microsc. **194**, 445 (1999).
[7] M. J. Gregor, P. G. Blome, J. Schöfer, and R. G. Ulbrich, Appl. Phys. Lett. **68**, 307 (1996).
[8] I. I. Smolyaninov, W. A. Atia, S. Pilevar, and C. C. Davis, Ultramicroscopy **71**, 177 (1998).
[9] D. A. Lapshin, E. E. Kobylkin, and V. S. Letokhov, Ultramicroscopy **83**, 17 (2000).
[10] T. R. Albrecht, P. Grütter, D. Horne, and D. Rugar, J. Appl. Phys. **69**, 668 (1991).
[11] U. Dürig, O. Züger, and A. Stalder, J. Appl. Phys. **72**, 1778 (1992).
[12] U. Dürig, H. R. Steinauer, and N. Blanc, J. Appl. Phys. **82**, 3641 (1997).
[13] G. T. Shubeita, S. K. Sekatskii, M. Chergui, G. Dietler, and V. S. Letokhov, Appl. Phys. Lett. **74**, 3453 (1999).
[14] Nanotechtools, Vignes 1, CH-1026 Echandens, Switzerland.
[15] F. J. Giessibl, Phys. Rev. B **56**, 16010 (1997).
[16] For a review, see, for example, G. N. Flerov and V. S. Barashenkov, Sov. Phys. Usp. **17**, 783 (1975).
[17] S. K. Sekatskii, G. T. Shubeita, and G. Dietler, poster presented at the 10th International STM Conference, Seoul, Korea, 18–23 July 1999 (unpublished).
[18] Apparent elongation of the holes, similar to the diagonal elongation in Fig. 5, was observed in some series of measurements (cf. Ref. 17). This can be explained by a combination of different reasons, including the peculiarities of nuclear filters preparation procedure (Ref. 16) and interaction of polarized light with the nanoholes in metal films [cf. C. Sönnichsen, A. C. Duch, G. Steininger, M. Koch, G. von Plessen, and J. Feldmann, Appl. Phys. Lett. **76**, 140 (2000)]; some effect of the piezoscanner drift also cannot be fully excluded.
[19] W. A. Atia and C. C. Davis, Appl. Phys. Lett. **70**, 405 (1997).
[20] A. G. T. Ruiter, K. O. van der Werf, J. A. Veerman, M. F. Garcia-Parajo, W. H. F. Rensen, and N. F. van Hulst, Ultramicroscopy **71**, 149 (1998).
[21] This simple but very general model is used throughout virtually all the papers describing tuning fork excitation; see, for example, Refs. 3–5 and 19. A profound discussion concerning the applicability of simple mechanical models for the force detection problem can be found in Ref. 11; see also Ref. 10.
[22] A more complicated model, which is given, for example, in A. Naber, J. Microsc. **194**, 307 (1999), also gives the similar results.
[23] Any textbook with an introduction to oscillatory motion, for example, J. B. Marion and S .T. Thornton, *Classical Dynamics of Particles and Systems*, 3rd ed. (Harcourt Brace Jovanovich, Orlando, FL, 1988).
[24] M. Heuberger, G. Dietler, and L. Schlapbach, Nanotechnology **5**, 12 (1994); J. Vac. Sci. Technol. B **14**, 1250 (1996).
[25] In particular, this implies that the optimal AFM scheme depends on the sample properties, see, for example, N. A. Burnham, G. Gremaud, A. J. Kulik, P.-J. Gallo, and F. Oulevey, J. Vac. Sci. Technol. B **14**, 1308 (1996), the same is valid for SNOM, and we are going to investigate the problem soon.
[26] S. K. Sekatskii, G. T. Shubeita, and G. Dietler, Appl. Phys. Lett. (submitted).
[27] D. A. Lapshin, V. N. Reshetov, S. K. Sekatskii, and V. S. Letokhov, JETP Lett. **67**, 263 (1998); Ultramicroscopy **76**, 13 (1999).
[28] D. P. Tsai and Y. Y. Lu, Appl. Phys. Lett. **73**, 2724 (1998).